Investigation of preheating method on joint strength of aluminium-stainless steel dissimilar welding using metal inert gas (MIG) process

IOP Conf. Series: Materials Science and Engineering **238** (2017) 012019 doi:10.1088/1757-899X/238/1/012019

Investigation of preheating method on joint strength of aluminium-stainless steel dissimilar welding using metal inert gas (MIG) process

M R Mohamad, L H Shah and M Ishak

Faculty of Mechanical Engineering, Universiti Malaysia Pahang, 26600 Pekan, Pahang, Malaysia

E-mail: luqmanhakim@ump.edu.my

Abstract. This study investigates AA6061-O and SUS304 dissimilar welding with preheating of stainless steel SUS304 prior to welding process. The welding method used was metal inert gas (MIG) with butt joint type weld. The mechanical strength was investigated using tensile test. Meanwhile, the macrostructure and microstructure of the specimens were analyzed using optical microscope, scanning electron microscopy (SEM) and energy dispersive spectroscopy (EDS). The tensile tests indicate that the preheated specimen with 90 °C have the maximum ultimate tensile strength of 111 MPa. In addition to that, the intermetallic compound (IMC) of the all the specimen was observed to be in the range of 1.59 µm to 10.8 µm. Fracture failures occur at the IMC interfaces on all specimen, where a thicker IMC layer consequently yields a lower tensile value. It can be concluded that the optimum parameters for AA6061-O to SUS304 welding can be achieved at 90 °C with 17.5 V welding voltage and 110 A welding current.

1. Introduction

Metal inert gas (MIG) welding is a prominent fusion welding method and is widely used in various industrial applications such as in shipbuilding, construction and automotive sector. Due to its long history, many researches have been done on its feasibility in various environments, and this is evident through the many international standards that have been established on MIG welding.

To meet new industrial demands, a new welding technique known as dissimilar welding was introduced. Such technique opens the possibilities to join metals of dissimilar alloy or material together to form a unique part. Dissimilar welding research have since seen many successful joining of different materials to aluminium, such as aluminium to steel [1], aluminium to copper [2], aluminium to magnesium [3] and aluminium to titanium [4].

Out of the many combinations, dissimilar welding between aluminium alloys and various steel alloys has been the most widely studied upon. This is primarily due to the high strength and toughness characteristics of steel alloys that compliments well with the low cost, light weight and corrosion resistant characteristic of aluminium alloys [5, 6]. However, such combination is difficult due to the near zero solubility and the stark contrast of the melting temperature between aluminium and steel. Consequently, this facilitates the formation of a notorious Fe_xAl_y brittle intermetallic (IMC) compound between the two metals during the joining process [7, 8]. Since these IMC layer formation is inevitable but adversely affects the weld strength, Kreimeyer and Sepold [9] have suggested that a weld joint with an IMC layer thickness of less than 10 µm is acceptable and can be considered mechanically sound.

To mitigate the formation of such brittle structure, several researches have proposed the use of preheating prior to the welding process. Recent researches by Kreimeyer and Vollertsen [10] and Bang et al. [11] have suggested a secondary heat source such as a tungsten inert gas (TIG) torch in order to preheat the steel counterpart prior to welding to enhance the joint strength. Other works also suggested the use of laser as a preheating source to enhance fusion and solid state welding between aluminium and steel [12–14]. These researches result in significant improvements to the joint strength due to the suppression of the deleterious IMC layer [15].

However, such additional preheating source set up is costly and complex. Shah et al. [16] conducted the preheating method using a mobile burner torch on tungsten inert gas (TIG) dissimilar welding of AA1100-SUS304 and AA6061-SUS304, respectively. The method proved to be simple, effective and cheap. Both results have shown an increase in the tensile strength of the joint when steel is preheated up to 150 ˚C.

2. Experimental Procedure

2.1 Materials

The base materials used in this study was a 2 mm thick aluminium alloy AA6061-O and stainless steel SUS304. Both metals were cut into plates with dimensions of 150×55×2 mm. The filler metals used for this study is ER4043. Table 1 shows the chemical composition (in wt%) for base metals AA6061 and SUS304 as well as filler material ER4043, respectively.

Table 1. Chemical composition (wt%) of AA6061, SUS304 and ER4043.

Materials	Zn	Ti	C	Mg	Si	Cr	Mn	Cu	Fe	Al
AA6061	0.021	0.028	-	0.775	0.643	0.191	0.073	0.236	0.303	Bal.
SUS304	-	-	0.06	-	0.397	17.90	1.010	0.210	Bal.	0.004
ER4043	0.1	0.2	-	0.05	<6.0	-	0.05	0.3	0.8	Bal.

2.2 Welding process

The joining process was carried out by using an automatic Dr Well DM-500EF MIG machine. The oxide layers on specimen surface were removed using a metal brush to prevent inclusion of impurities in the weld joint. They were then carefully cleaned using acetone and left to dry to remove dirt and grease.

Table 2. Fixed and varied MIG welding parameter

Welding parameter	Value
Welding speed	4 mm/sec
Preheating temperature	90 ˚C, 180 ˚C, 270 ˚C
Welding voltage	17 V, 17.5 V, 18 V
Welding current	105 A, 110 A, 115 A

Details of the fixed and varied welding parameters are presented in table 2. Through preliminary tests, no sound welds can be formed using lower or higher values of welding voltage and current. Welding with the parameters mentioned in table 2 without preheating also yielded unsuccessful joints. After the welding set up and just prior to the welding process, the stainless-steel counterpart was preheated using a commercially available gas burner torch up to the desired temperature. The temperature was monitored closely using a mobile Center 300 Series digital thermometer with surface probe. Once the desired temperature was reached, the welding process commenced.

2.3 Mechanical and microstructural analysis

In order to investigate the specimen joint strength, tensile tests were conducted using the Shimadzu Universal AG-X tensile test machine. The dimension for the tensile specimen was cut using an electrical discharge machining (EDM) wire cut according to the ASTM-E8 standard. Figure 1 shows the dimension (in millimeters) for the tensile specimen. The weld joint is to be located at the middle of the dog bone shape.

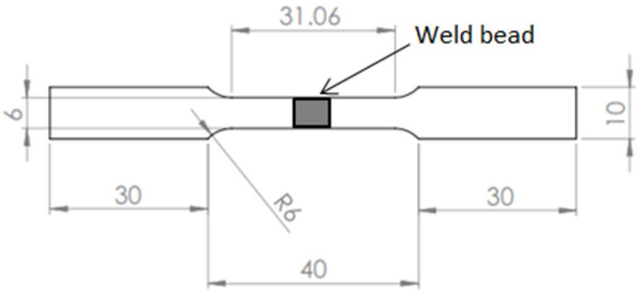

Figure 1. Tensile specimen dimensions (in mm).

For the microstructure analysis, the specimens were ground using 240, 320, 400 and 600 grit papers in that order and polished using 6 µm and 0.05 µm polishing plates to remove scratches on the surface to be observed. To reveal the grain boundaries, they are finally etched by dabbing a cotton bud immersed in an HF aqueous solution for the stainless-steel region, and a separate cotton bud immersed in Keller's reagent for the aluminium counterpart, respectively, in ambient temperature. Microstructure and elemental analysis of the specimen were observed using optical microscope, scanning electron microscopy (SEM) and energy dispersive X-ray spectroscopy (EDX).

3. Results and Discussion

3.1 Welding appearance

Figure 2 shows the best surface appearance of the welded specimens for each preheating temperature group. From the figure below, it can be seen that sound weld joints with minor defects can be obtained from the process. A better weld bead consistency can be observed from figure 2(a) using the 90 ˚C preheating temperature (sample 2), but better wetting can be observed for sample 4 and sample 9.

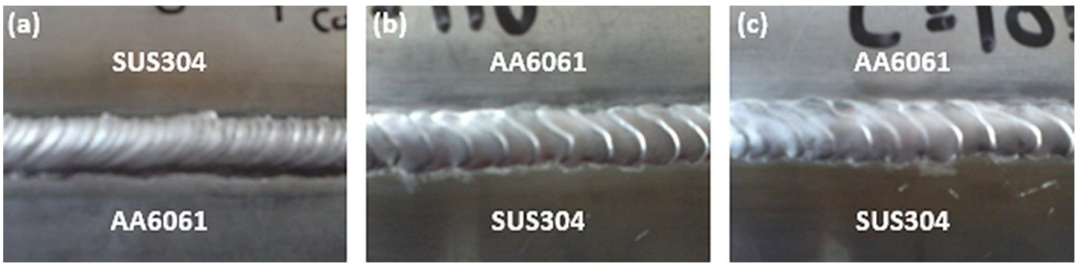

Figure 2. Surface appearance of the welded specimens for (a) 90 ˚C (sample 2), (b) 180 ˚C (sample 4) and (c) 270 ˚C (sample 9).

3.2 Tensile test

Figure 3 shows the side and top view of the fractured tensile test specimen. A more detail view of the weld bead before and after the fracture can be observed in figure 4. It can be seen in figure 4(a) that the welding process yielded a welding-brazing joint; the aluminium side combined with the aluminium filler to create a welding joint, whereas the ER4043 filler only brazed at the contact surface of the steel side. After fracture, figure 4(b) clearly shows that the line of fracture originates from the stainless steel and aluminium brazing boundary, i.e. the brittle intermetallic layer, indicating a brittle fracture mode.

The result of the tensile tests with the respective parameters is shown in table 3. The heat input from the MIG torch was calculated using the equation below [17]:

$$J = c \times UI \quad (1)$$

where J is the heat input (kJ/mm), c is the constant value of coefficient of welding efficiency over travel speed (mm/s), μ/V, U is the current (A) and I is the voltage (V).

From the data collected in the table, a graph of tensile strength versus preheating level and specimen number was plotted, as shown in figure 5. From the figure, it can be seen that the highest tensile strength is 111 MPa for sample 2 at preheating level 90 ˚C with 17.5 V welding voltage and 110 A welding current. This value is 90% of the tensile strength of the AA6061-O base metal (124 MPa). On the other hand, the lowest tensile strength value obtained was from sample 7 with 61 MPa using preheating temperature of 270 ˚C, voltage of 17 V and current of 110 A.

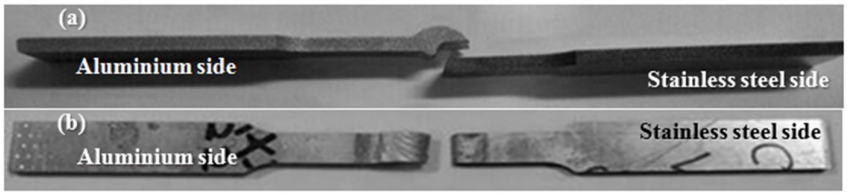

Figure 3. Fractured tensile specimen from the (a) side view, and (b) top view.

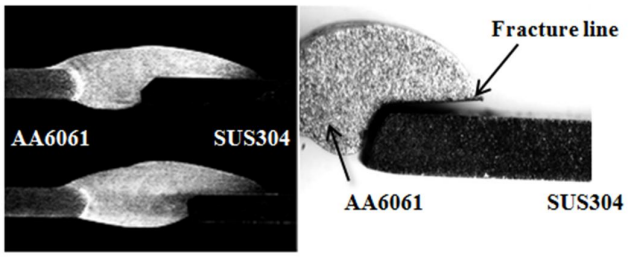

Figure 4. Cross sectional view of weld bead (a) as welded, and (b) after tensile testing.

Table 3. Tensile test results for all specimens.

Sample	Preheating(°C)	Voltage(V)	Current(C)	Heat input(kJ/mm)	Tensile strength(MPa)
1	90	17	105	1785*c*	104.53
2	90	17.5	110	1925*c*	111.27
3	90	18	115	2070*c*	66.46
4	180	17	115	1955*c*	95.04
5	180	17.5	105	1837.5*c*	88.34
6	180	18	110	1980*c*	89.28
7	270	17	110	1870*c*	60.53
8	270	17.5	115	2012.5*c*	80.97
9	270	18	105	1890*c*	82.67

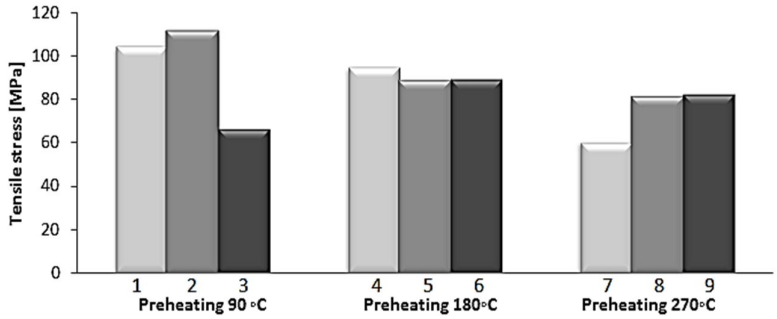

Figure 5. Tensile strength result.

3.3 Microstructure analysis

Figure 6 shows the microstructure morphology of the welded joint using an optical microscope at a low magnification (figure 6(a)-(c)) and at a high magnification (figure 6(d)-(f)), respectively. A mixed region can be observed between the weld zone and the aluminium base metal (figure 6(a)). On the other hand, a clear thin boundary between the weld zone and stainless steel base metal can be seen (figure 6(b)-(c)).

With a higher magnification, the transition between weld zone and heat affected zone (HAZ) of aluminium can be seen at the aluminium side (figure 6(d)). Coarse grains can be seen on the left side of figure, indicating that HAZ experienced thermal cycle without deformation. On the contrary, figure 6(e)-(f) show the existence of a thin inter metallic compound (IMC) layer on the inner and top faying surface of the steel sheet (inner and top IMC layer), respectively.

To better understand the IMC layer and the region surrounding it, the region is further examined using a scanning electron microscopy (SEM) and energy dispersive X-ray spectroscopy (EDX). Figure 7 shows the result of the SEM analysis at the inner side and top side of the bonded aluminium-steel surface. Due to the inconsistency of the thickness, several points were taken to determine the thickness range. The IMC thickness range for sample 2 was measured to be between 1.59 and 10.8 µm in size, indicating that a mechanically sound joint was achieved.

A line elemental analysis of the IMC layer region was conducted using EDX and its count-per-second versus position graphs of the main elements are shown in figure 8. From the individual elemental spectrums, it is evident that the left side of the analysis region (fig.8(a)) is dominated by aluminium and magnesium (fig.8(b)-(c)), whereas iron is mostly present on the right side (fig.8(d)). As for the IMC layer, it consists of aluminium, magnesium, silicon and carbon. Apart from the main elements of base metals, magnesium and silicon (fig.8(c) and (e)) are present primarily from the aluminium base metal and filler metal. However, since there is low carbon content in the initial set up, it is still unclear as to how carbon emerged in the IMC content. It can be assumed that the abrupt increase of carbon at the IMC layer (fig.8(f)) is primarily due to hydro carbon contaminants present at the faying surface of each material and at the filler metal surface. Further study is needed to clarify this issue.

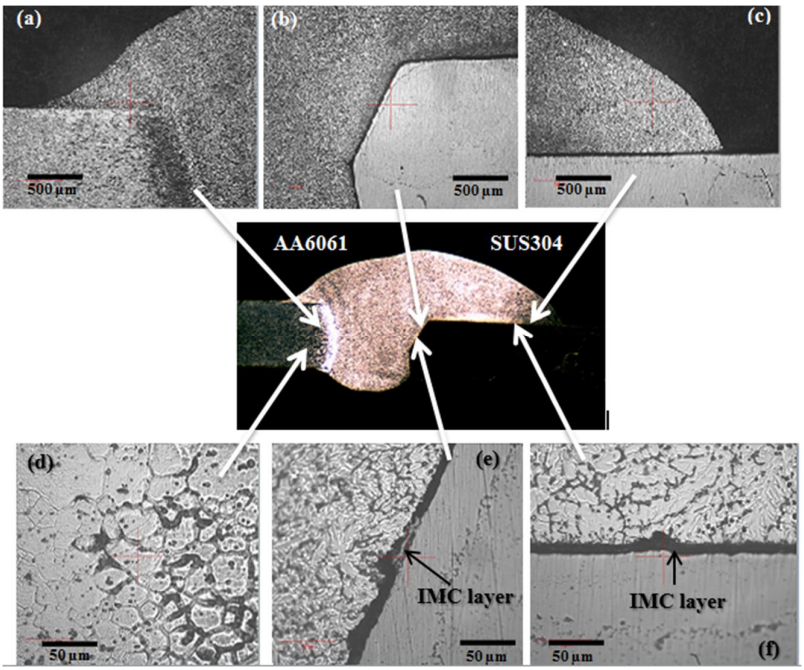

Figure 6. Microstructure morphology of the welded joint at 5× magnification; (a) aluminium joint, (b) inner steel joint, (c) top steel joint and at 50× magnification; (d) transition region of aluminium, (e) inner IMC layer, (f) top IMC layer.

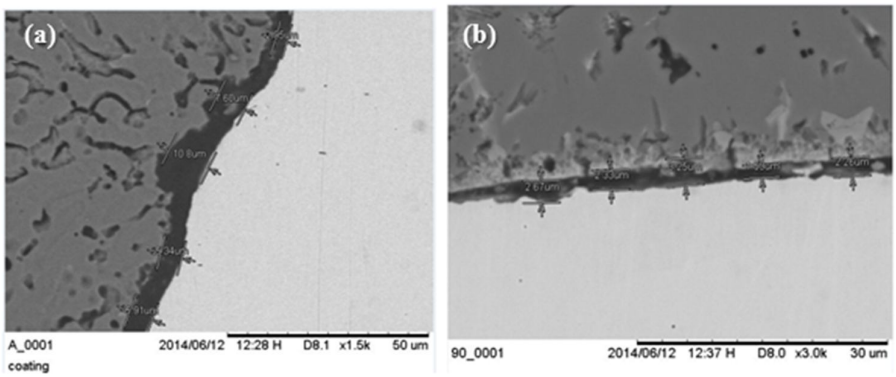

Figure 7. IMC thickness analysis at the (a) inner steel region and (b) top steel region.

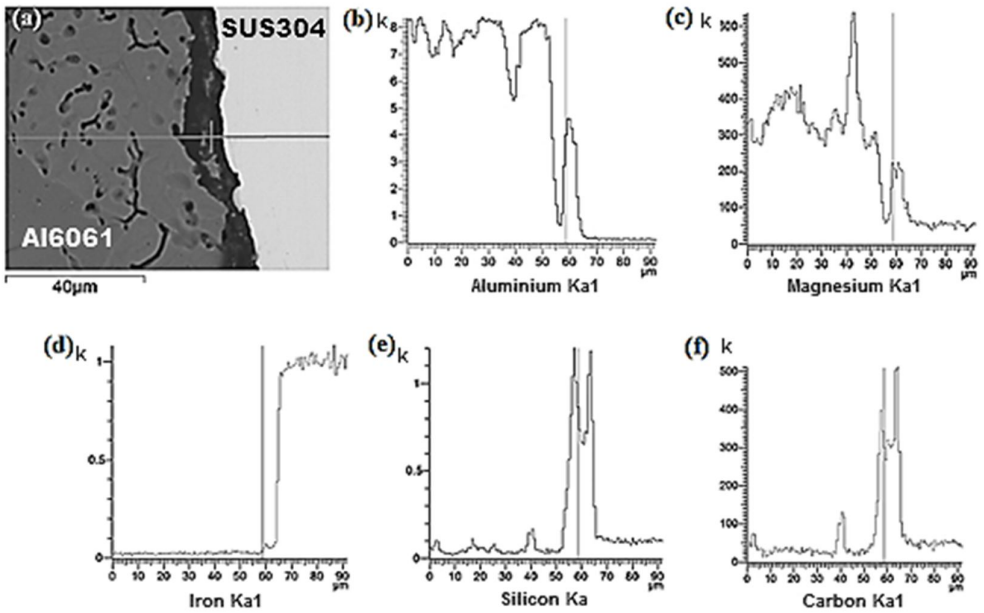

Figure 8. EDX line elemental analysis of the IMC region with individual elemental spectrums; (a)analyzed region; (b)aluminium; (c)iron; (d)magnesium; (e)silicon; (f)carbon.

The premise of the preheating method is to enhance diffusion between the base metals at a shorter duration and lower heat input. The IMC thickness under diffusion control process is governed by:

$$X = K\sqrt{t} \tag{2}$$

and

$$K = K_o \exp\left(-\frac{Q}{RT}\right) \tag{3}$$

where X is the IMC thickness (mm), t is the time (s) for diffusion, K_o is a constant, Q is the activation energy (J) for the growth of the layer, R is gas constant and T is the absolute temperature (K) [18, 19]. It is postulated that preheating on the stainless-steel counterpart provides additional energy to the system to surpass the threshold of Q in order to initiate IMC formation with lower heat input. With lower excessive heat input introduced to the system during the welding process, a shorter duration can be achieved, thus, from the equation (2), a thinner IMC can be formed.

The correlation between tensile strength, IMC thickness and the welding parameters can be explained as follows. As shown in figure 2, the samples with the best weld appearance have shown moderate heat input in the mid-range between the lowest and highest heat input, 1785*c* kJ/mm and 2070*c* kJ/mm, respectively. However, contrary to sample 2, tensile strength for both sample 4 and sample 9 show low tensile strength compared to other samples. This implies that despite the moderate heat input from the MIG torch which facilitates the wetting and consolidating process, the higher preheating temperature (180 °C and 270 °C respectively) of both samples may have caused the brittle IMC layers to grow thicker and cause detrimental effects on the samples' mechanical property. A general trend of decreasing tensile strength as preheating temperature increases can also be seen in figure 5, except for sample 3. Having the highest heat input (2070*c* kJ/mm), the excess heat input in sample 3 may have also caused further IMC growth and therefore a low tensile strength is produced.

4. Conclusion

Dissimilar metals joints between aluminum alloy AA6061-O and stainless steel SUS304 were successfully joined by MIG welding with preheating on the stainless-steel specimen before welding process. Major conclusions of this study could be summarized as follows:

i. All specimen yielded quality joints with minor defects.

ii. Fracture failure occurs at the IMC interface on all specimens. The preheated specimen with 90 °C preheating obtained the maximum ultimate tensile strength of 111 MPa.
iii. The IMC of the specimen with highest tensile strength was observed to be in the range of 1.59 µm to 10.8 µm.
iv. EDX analysis show that the IMC mainly consists of the base metal elements as well as contaminants.
v. The optimum parameters for dissimilar welding of AA6061-O and SUS304 can be achieved at 90 °C with 17.5 V welding voltage and 110 A welding current.

Acknowledgement
The authors would like to thank Universiti Malaysia Pahang for the research funding through RDU121409 and to the university staffs that have help to make this research a success.

References
[1] Rathod M J, Kutsuna M 2004 Joining of Aluminum Alloy 5052 and Low-Carbon Steel by Laser Roll Welding *J Weld* 83:16–26.
[2] Saeid T, Abdollah-zadeh A, Sazgari B 2010 Weldability and mechanical properties of dissimilar aluminum–copper lap joints made by friction stir welding *J Alloys Compd* 490:652–655.
[3] Kwon Y J, Shigematsu I, Saito N 2008 Dissimilar friction stir welding between magnesium and aluminum alloys *Mater Lett* 62:3827–3829.
[4] Dressler U, Biallas G, Alfaro Mercado U 2009 Friction stir welding of titanium alloy TiAl6V4 to aluminium alloy AA2024-T3 *Mater Sci Eng A* 526:113–117.
[5] Fukumoto S, Tsubakino H, Okita K 2000 Amorphization by friction welding between 5052 aluminum alloy and 304 stainless steel *Scr Mater* 42:807–812.
[6] Staubach M, Juttner S, Fussel U, Dietrich M 2008 Joining of steel-aluminium mixed joints with energy-reduced GMA processes and filler materials on an aluminium and zinc basis *Weld Cut* 7:30–38.
[7] Dharmendra C, Rao K P, Wilden J, Reich S 2011 Study on laser welding–brazing of zinc coated steel to aluminum alloy with a zinc based filler *Mater Sci Eng A* 528:1497–1503.
[8] Qiu R, Iwamoto C, Satonaka S 2009 The influence of reaction layer on the strength of aluminum/steel joint welded by resistance spot welding *Mater Charact* 60:156–159.
[9] Kreimeyer M, Sepold G 2002 Laser steel joined aluminium-hybrid structures. Proc. Int. Congr. Appl *Lasers Electro-Optics* 2002
[10] Kreimeyer M, Vollertsen F 2006 Gap tolerant joining of aluminium with steel sheets using the hybrid technique. In: Proc. Int. Congr. Appl. *Lasers Electro-Optics 2006*. Arizona, USA, pp 947–952
[11] Bang H, Bang H, Jeon G 2012 Gas tungsten arc welding assisted hybrid friction stir welding of dissimilar materials Al6061-T6 aluminum alloy and STS304 stainless steel. Mater Des 37:48–55.
[12] Qin G, Lei Z, Su Y 2014 Large spot laser assisted GMA brazing–fusion welding of aluminum alloy to galvanized steel *J Mater Process Technol* 214:2684–2692.
[13] Qin G, Su Y, Wang S 2014 Microstructures and properties of welded joint of aluminum alloy to galvanized steel by Nd:YAG laser + MIG arc hybrid brazing-fusion welding *Trans Nonferrous Met Soc China* 24:989–995.
[14] Merklein M, Giera A 2008 Laser assisted friction stir welding of drawable steel-aluminium tailored hybrids *Int J Mater Form* 1:1299–1302.
[15] Shah L H, Ishak M 2014 Review of Research Progress on Aluminum–Steel Dissimilar Welding *Mater Manuf Process* 29:928–933.
[16] Shah L H, Yusof A S M, Ishak M 2013 Investigation of heat treatment on weld joint quality of stainless steel and aluminium dissimilar welding *Proc. 16th Int. Conf. Adv. Mater. Process. Technol.*
[17] Nowacki J, Rybicki P 2005 The influence of welding heat input on submerged arc welded

duplex steel joints imperfections *J Mater Process Technol* 164–165:1082–1088.
[18] Kobayashi S, Yakou T 2002 Control of intermetallic compound layers at interface between steel and aluminum by diffusion-treatment *Mater Sci Eng A* 338:44–53.
[19] Borrisutthekul R, Yachi T, Miyashita Y, Mutoh Y 2007 Suppression of intermetallic reaction layer formation by controlling heat flow in dissimilar joining of steel and aluminum alloy. *Mater Sci Eng A* 467:108–113.